

Distributionally Robust Optimization and Invariant Representation Learning for Addressing Subgroup Underrepresentation: Mechanisms and Limitations

Nilesh Kumar*, Ruby Shrestha*, Zhiyuan Li and Linwei Wang

Rochester Institute of Technology, NY, USA

Abstract. Spurious correlation caused by subgroup underrepresentation has received increasing attention as a source of bias that can be perpetuated by deep neural networks (DNNs). Distributionally robust optimization has shown success in addressing this bias, although the underlying working mechanism mostly relies on upweighting under-performing samples as surrogates for those underrepresented in data. At the same time, while invariant representation learning has been a powerful choice for removing nuisance sensitive features, it has been little considered in settings where spurious correlations are caused by significant underrepresentation of subgroups. In this paper, we take the first step to better *understand* and *improve* the mechanisms for debiasing spurious correlation due to subgroup underrepresentation in medical image classification. Through a comprehensive evaluation study, we first show that 1) generalized reweighting of under-performing samples can be problematic when bias is not the only cause for poor performance, while 2) naive invariant representation learning suffers from spurious correlations itself. We then present a novel approach that leverages robust optimization to facilitate the learning of invariant representations at the presence of spurious correlations. Finetuned classifiers utilizing such representation demonstrated improved abilities to reduce subgroup performance disparity while maintaining high average and worst-group performance.

Keywords: Spurious correlations · DRO · Invariant representations.

1 Introduction

As deep neural networks (DNNs) continue to demonstrate successes in various tasks [7,18], their potential to generate and perpetuate bias also received growing attention [16,14]. One source of biases being increasingly discussed is the presence of *spurious correlation* due to *subgroup underrepresentation*, where features irrelevant to a task happen to co-exist with a decision label in the majority of the samples (*bias-aligning* samples) whereas samples that do not exhibit such correlation are underrepresented (*bias-conflicting* samples). Examples may include the presence of treatment features in positive disease samples (*e.g.*, the

* These authors contributed equally to this work

presence of drain as a treatment was observed in the majority of pneumothorax samples in CXR-14 chest X-rays [16]), or a higher prevalence of disease in certain demographic subgroups (*e.g.*, malignant skin cancer was more commonly reported in lighter skin tones [9]). With the standard *empirical risk minimization* (ERM), [23], the DNN is trained to exploit such spurious correlation for reducing the *average* loss of all training samples [14]. Such DNN will struggle with bias-conflicting subgroups.

Most works have approached this bias from the lens of distributionally robust optimization (DRO), a classic optimization concept that focuses on minimizing worst-case losses over possible test distributions [1]. The recent integration of DRO into DNN was done by describing possible test distributions with importance sampling of the observed subgroups [20]: the group DRO (GDRO) is then solved by iteratively optimizing the importance weights of all subgroups to maximize the DNN loss while optimizing the DNN to minimize such worst-case loss. This min-max formulation enables GDRO to pay equal or even greater attention to underrepresented subgroups, although it requires the subgroup labels to be known *a priori*. To remove this need, various approaches have followed to identify bias-conflicting samples by, for instance, considering high-loss samples in a biased model [12,15] or clustering the biased representations [22]. At the core of all of these approaches is *a generalized re-weighting scheme to achieve DRO, i.e.*, minimizing worst-case losses by upweighting the contribution from bias-conflicting subgroups. A fundamental working mechanism behind these approaches, however, assumes that high training loss of the ERM model can be used to determine the upweighting of bias-conflicting samples. While this was shown to be empirically effective on carefully designed benchmark datasets where spurious correlation is the dominating cause for poor performance, it is not clear how this working mechanism may generalize in real-world datasets where the high loss of a training sample may be due to other challenges such as the difficulty to extract discriminative semantics for certain disease categories.

In parallel, *invariant representation learning* has been a mainstream approach for removing confounding semantics not responsible for a task, especially for training DNNs that can adapt or generalize across domains [4]. It has also been widely used in *fair representation learning* to obfuscate sensitive group attributes from latent representations [3,13,17,21,27]. These works however either do not deal with spurious correlations due to underrepresented subgroups, deal with limited spurious correlation resulting from insubstantial bias ratio, or make the assumption that there exists a curated subset of data (for example, a training class) that does not exhibit subgroup underrepresentation. Within limited attempts of using invariant representations to handle spurious correlation, there are often specific assumptions of what may be the spurious factors (*e.g.* texture of the image) and thus lacks generality [24]. To the best of our knowledge, there is very limited work on general purpose methods to learn representations invariant to spurious correlations [26]. This leaves another intriguing open question: what may be the role and challenges of invariant representation learning in addressing spurious correlation caused by underrepresentation?

In a nutshell, despite increasing interest in DNN fairness and bias [25], approaches to specifically address spurious correlation caused by subgroup representation have been limited in medical image classification [8,22] and their working debiasing mechanisms and limitations are not well understood. In this paper, we take the first step to better *understand* and *improve* the debiasing mechanism for addressing spurious correlation in medical image classification. To understand the potential mechanisms for debiasing and corresponding limitations (Section 2), we conduct a comprehensive evaluation study in which we examine the aforementioned families of approaches to address spurious correlation on two skin lesion datasets. Results suggested that 1) generalized reweighting based on under-performing samples can be problematic in real-world datasets where bias is not the only cause for low performance, and 2) invariant representation learning suffers from spurious correlation and subgroup underrepresentation itself. As a first step to address these observed limitations, we further show that – while GDRO in itself has little influence on representation learning – its combination with domain adversarial loss can enable invariant representation learning in the presence of spurious correlation (Section 3). Fine-tuning the classifier using such representation on balanced validation dataset, as inspired by deep feature reweighting (DFR) [10], further improved the reduction of subgroup disparity while achieving high average performance.

2 Assessing Debiasing Mechanisms

2.1 Methodology

Data: We consider two skin lesion datasets that exhibit different levels of complexity in the underlying tasks, biases, and the number of subgroups.

ISIC [2]: The spurious correlation in ISIC was originally caused by the presence of bandages in benign examples and the absence of bandages in malignant examples [5]. Here we introduce a small subgroup of such malignant samples in the training to assess bias due to such underrepresentation. This is achieved by artificially adding bandages to malignant examples using the segmentation masks for bandages from [19]. Table 1 shows the distribution of training data.

Fitzpatrick [6]: As summarized in Table 1, in Fitzpatrick, there is a higher prevalence of malignant skin cancers in lighter skin tones (Fitzpatrick skin type 1-2) versus a higher prevalence of non-neoplastic lesions in darker skin tones (Fitzpatrick skin type 5-6). This shift of label distribution among skin-type subgroups may create a bias of under-diagnosis of malignant skin cancers in individuals with darker skin tones. To focus on this potential bias, we reduce overall skin-type imbalance by downsampling samples from skin types 1-4, while maintaining the same label distribution within each skin-type subgroup.

Models: We consider three families of models to provide complete coverage of existing strategies focused on DRO and/or representation learning.

Generalized reweighting approaches: Representing approaches using known subgroup labels, we consider simple importance weighting (with fixed subgroup

Table 1. Subgroup distribution in training. Bias-conflicting subgroups shaded gray.

Dataset	Subgroup Distribution in Training Data						
ISIC	Benign-no bandage	Benign-bandage	Malignant-no bandage		Malignant-bandage		
	4843	4890	5205		100		
Fitzpatrick	Skin type	1	2	3	4	5	6
		Class					
	Benign	15.07%	13.96%	14.36%	13.20%	10.37%	6.93%
	Malignant	15.37%	15.43%	13.78%	10.82%	9.59%	9.61%
Non-neoplastic	69.56%	70.61%	71.86%	75.98%	80.04%	83.46%	

weights) and GDRO [20] (with dynamic weights). Representing approaches with unknown subgroups, we consider JTT [12] where bias-conflicting samples are identified as under-performing samples in ERM, followed by upweighting.

Invariant representation learning: We consider a classic invariant representation learning strategy that removes domain information from the latent representation by a reversal gradient layer (known as domain adversarial training of neural networks/DANN) [4]. We use the bias-inducing factor as the domain, *i.e.* the presence and absence of bandage in ISIC and the skin types in Fitzpatrick. We also consider the only existing general-purpose invariant representation learning approach reported for spurious correlation, where contrastive learning is used to push representations of samples of the same class closer (CnC) [26].

Separated representation & decision-boundary learning: We include deep feature reweighting (DFR) [10] that first obtains biased ERM representation, and then re-trains a classifier using such representations on a balanced validation set.

Evaluation Metrics: We consider three types of evaluation metrics.

To *evaluate bias in representations*, we leverage self-organizing maps (SOM) [11] to cluster and visualize the latent representations. We also adopt a quantitative metric of *cluster purity* as a surrogate measure of biases in the latent representations. This is motivated by the concept that, in an ideal scenario, an unbiased representation should discard and thus not be separable by spuriously-correlated features.

To *evaluate bias in the decision boundary*, we consider two general types of quantitative metrics: 1) test performance for the worst-performing subgroup, the anticipated bias-conflicting subgroups, and averages across all subgroups; 2) The performance disparity (Δ) among all subgroups: in ISIC, this is measured as performance difference between worst-performing subgroups to best-performing subgroups ($\Delta_{best-worst}$) and to group-average performance ($\Delta_{avg-worst}$), respectively. In Fitzpatrick, because the number of subgroups is large (3×6), this is measured by Δ between best- and worst-performing subgroups in each class: malignant, non-neoplastic, and benign (Δ_{mn} , Δ_{nn} , Δ_{bg}) as well as their average (Δ_{avg}).

To *assess the debiasing mechanisms*, for generalized reweighting with and without known subgroups, we track their importance weights, or the subgroups

	Avg	Worst	Malignant Bandage	$\Delta_{best-worst}$	$\Delta_{avg-worst}$
ERM	0.803 \pm 0.005	0.556 \pm 0.072	0.556 \pm 0.072	0.443 \pm 0.072	0.246 \pm 0.066
Important weighting	0.793 \pm 0.011	0.593 \pm 0.040	0.593 \pm 0.040	0.406 \pm 0.040	0.200 \pm 0.030
JTT	0.790 \pm 0.011	0.550 \pm 0.051	0.550 \pm 0.051	0.450 \pm 0.051	0.240 \pm 0.041
DANN	0.843 \pm 0.005	0.730 \pm 0.017	0.730 \pm 0.017	0.266 \pm 0.023	0.113 \pm 0.011
DFR	0.871 \pm 0.004	0.758 \pm 0.008	0.865 \pm 0.010	0.232 \pm 0.010	0.112 \pm 0.010
GDRO	0.846 \pm 0.011	0.760 \pm 0.017	0.763 \pm 0.015	0.240 \pm 0.017	0.086 \pm 0.005
GDRO with group adjustment	0.866 \pm 0.005	0.786 \pm 0.011	0.803 \pm 0.020	0.213 \pm 0.011	0.080 \pm 0.005
Proposed method	0.863 \pm 0.005	0.800 \pm 0.000	0.813 \pm 0.023	0.190 \pm 0.000	0.063 \pm 0.005

Table 2. Accuracy of benign *vs.* malignant classification on ISIC. Malignant samples with a bandage is the underrepresented bias-conflicting group as expected from Table 1. Columns 2-4 list accuracy of averaged and individual subgroups. Columns 5-6 measure the performance disparity among subgroups. Best performance is shaded gray, with bolded performance closely behind.

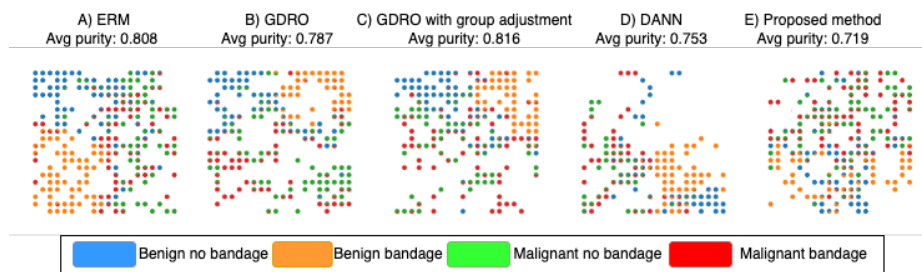


Fig. 1. SOM plots and their averaged subgroup purities.

identified for up-weighting, respectively. For learning invariant representations, we track the accuracy of the domain classifier in removing spurious features.

2.2 Experiments and Results

Following convention [20,26], we used ResNet-50 from torch-vision with pre-trained weights from Imagenet. We used held-out validation set to choose the best model unless the method is using the validation set for fine-tuning (*e.g.*, DFR).

ISIC: As summarized in Table 2, with ERM, the DNN suffered from a significant performance drop for the bias-conflicting subgroup (malignant samples with bandage). This bias is also evident in the SOM (Fig 1A), which shows clearly separated subgroups and a relatively high purity score.

Generalized reweighting approaches: Simple importance weighting (to equally weight all subgroups) improved the test accuracy on the bias-conflicting group but to a limited extent. GDRO more significantly improved the test performance of the bias-conflicting subgroup. Interestingly, a closer inspection on the subgroup weights obtained by the GDRO (Figure. 2A) showed that GDRO actually upweighted the two non-bandage subgroups. Evidently, with group-based average loss, the underrepresented group is already upweighted in GDRO which quickly resulted in a lower loss at the early stage of training. As such,

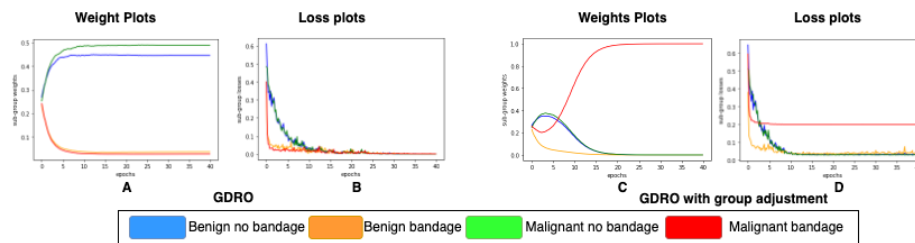


Fig. 2. Weight and loss plots for GDRO with and without group adjustment.

the other two non-bandage subgroups unexpectedly became the higher-loss subgroups (Figure. 2B) and were upweighted. The separation of subgroups in the SOM remained similar to ERM with slightly reduced purity (Fig 1B).

Facing this unexpected working mechanism of GDRO, we further experimented with a version of GDRO with *group adjustment* [20]: this adds an additional term of $\frac{1}{\sqrt{N_s}}$ to the subgroup loss where N_s is the size of a subgroup. As expected, this term dominates the loss used to optimize the weights (Figure. 2D) and resulted in a heavy upweighting of the bias-conflicting group (Figure. 2C). This resulted in further improvement on this subgroup. Clustering of the latent representation and its purity however remained similar to the ERM (Fig 1C).

These results revealed that the use of group adjustment played a significant role in the weighting mechanism of GDRO. Without this, the upweighting was influenced by other factors contributing to low performance and the overall results appeared to be adversely affected.

Invariant representation approaches: DANN was trained with upsampling of the underrepresented subgroup. Its performance was better than simple importance weighting, but inferior to GDRO. A closer look at the obtained representation clusters (Fig 1D) and the behaviour of the domain classifier (Figure 3A) suggested that DANN was not successful in removing bandage information from the bias-aligning subgroup (benign with bandage). This failure suggested that domain-invariant representation learning also suffers from spurious correlations.

Approaches without subgroup labels: For the remaining models that do not require the use of subgroup labels, the performance was suboptimal. JTT showed minor improvement over ERM, while CnC under-performed than ERM (results thus not included). Common to both approaches was the reliance on a biased ERM model to identify bias-conflicting examples. A closer inspection showed that, among the under-performing samples selected from the biased ERM, only 1.05-2.75% belonged to the bias-conflicting subgroup. This explained why the subsequent learning approaches may not be successful. Finally, DFR achieved an impressive average performance as well as on the bias-conflicting subgroup, albeit at the expense of creating a new worst-performing subgroup.

Fitzpatrick: Table 3 shows the average AUC, worst-AUC among all 18 subgroups, and AUCs for four selected subgroups that are most indicative of the bias present: with ERM, the subgroups with darker skin tones are disadvantaged in

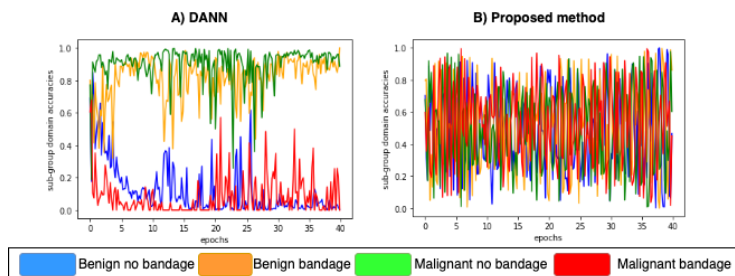


Fig. 3. Subgroup accuracy of domain classifier in A) DANN and B) as proposed.

malignant cancer detection (MN-56, AUC of 0.81 *vs.*, 0.88 for MN-12), whereas the subgroups with lighter skin tones are disadvantaged in non-neoplastic lesion detection (NN-12, AUC of 0.78 *vs.*, 0.86 for NN-56). This disparity in performance is perfectly associated with the subgroup label distributional shifts shown in Table 1, an intriguing non-artificial bias that may be challenging to address.

The trend of performance of all models was similar to that observed in ISIC with some distinction. JTT and CnC continued to under-perform and their results are not included. Unlike on ISIC, here both DANN and DFR obtained negligible or even negative gains over ERM. In comparison, various reweighting strategies were all effective in addressing the bias against MN-56, albeit 1) at the expense of decreased average AUC, and 2) ineffective in addressing the bias against NN-12. The measures of performance disparity within and averaged across classes (Table 4) suggested the same trend.

Note that the worst-performance subgroups from all models were different from the bias-conflicting subgroups, which may be why this particular bias was challenging to remove.

3 Improving the Debiasing of Spurious Correlations

Methodology: The investigations in Section 2 provided two important findings. First, the reliance on low training performance for identifying or upweighting bias-conflicting samples may face challenges where bias is not the only cause for under-performing samples. Second, while invariant representation in concept appears a natural candidate for removing confounders, its learning ironically also suffers from spurious correlation caused by underrepresentation. This raises a critical question: is our best hope upweighting known bias-conflicting subgroups?

We re-examine DANN’s failure to confuse the domain classifier on the bias-aligned subgroups (Fig. 3A). A possible explanation is that the main task classifier was exploiting spurious correlations and overpowers the domain classifier. Based on this, we hypothesize that a robust main classifier with a reduced tendency to exploit spurious correlation may better support DANN to learn representations invariant to spurious correlations. To this end, we propose to optimize the main classifier in DANN with GDRO and, with the learned invariant representation, fine-tune only the classifier on a small validation set.

	Average	Worst	MN-12	MN-56	NN-12	NN-56
ERM	0.810 ± 0.000	0.617 ± 0.040	0.878 ± 0.008	0.810 ± 0.018	0.777 ± 0.010	0.855 ± 0.005
Importance weighting	0.803 ± 0.015	0.673 ± 0.035	0.878 ± 0.010	0.853 ± 0.008	0.780 ± 0.001	0.853 ± 0.010
DANN	0.787 ± 0.006	0.607 ± 0.015	0.857 ± 0.010	0.758 ± 0.014	0.785 ± 0.005	0.800 ± 0.015
DFR	0.790 ± 0.010	0.660 ± 0.036	0.863 ± 0.003	0.813 ± 0.020	0.778 ± 0.008	0.828 ± 0.010
GDRO	0.800 ± 0.010	0.640 ± 0.030	0.868 ± 0.008	0.848 ± 0.055	0.788 ± 0.012	0.825 ± 0.020
GDRO with group adjustment	0.780 ± 0.010	0.647 ± 0.006	0.852 ± 0.008	0.877 ± 0.016	0.782 ± 0.015	0.788 ± 0.022
Proposed method	0.810 ± 0.000	0.680 ± 0.026	0.883 ± 0.003	0.837 ± 0.003	0.803 ± 0.003	0.830 ± 0.009

Table 3. AUC of benign, malignant, and non-neoplastic skin lesion classification on Fitzpatrick. MN-12/-56: malignant with skin type 1-2 / 5-6. NN-12/56: non-neoplastic with skin type 1-2 / 5-6. MN-56 and NN-12 are the primary bias-conflicting subgroups.

	Δ_{mn}	Δ_{nn}	Δ_{bg}	Δ_{avg}
ERM	0.140 ± 0.026	0.083 ± 0.015	0.223 ± 0.032	0.149 ± 0.020
Importance Weighting	0.073 ± 0.021	0.080 ± 0.020	0.153 ± 0.006	0.102 ± 0.010
DANN	0.250 ± 0.036	0.040 ± 0.010	0.233 ± 0.015	0.174 ± 0.018
DFR	0.157 ± 0.040	0.053 ± 0.006	0.150 ± 0.030	0.120 ± 0.021
GDRO	0.090 ± 0.087	0.053 ± 0.025	0.197 ± 0.055	0.113 ± 0.055
GDRO with group adjustment	0.053 ± 0.015	0.030 ± 0.010	0.163 ± 0.021	0.082 ± 0.004
Proposed method	0.090 ± 0.010	0.037 ± 0.006	0.117 ± 0.031	0.081 ± 0.008

Table 4. Difference in AUCs between best- and worst-performing subgroups in each class, from left to right: malignant, non-neoplastic, benign, and averaged.

Experiments and Results: On ISIC, the proposed model was successful in extracting invariant representations, evidenced both by the confused DANN domain classifier (Figure 3B) and the substantially reduced SOM purity (Fig 1E). After fine-tuning this invariant representation on a small balanced validation set as used in DFR, the proposed approach achieved the highest worst-performance among all models considered (Table 2). Its performance on the bias-conflicting subgroup was better than GDRO with group adjustment, and its average performance on par. Note that while DFR exhibited a stronger average performance on the bias-conflicting subgroup, its worst-group performance was much lower. In comparison, the proposed method was the most successful in reducing subgroup disparity (last two columns in Table 2) with strong average performance.

Evidence of improved invariant representations was similar on Fitzpatrick (results shown in supplemental materials).

As summarized in Tables 3-4, compared to reweighting methods, the fine-tuned classifier as proposed was the only one that was able to reduce the bias against NN-12, and delivered the best worst-group as well as average performance. Overall, its performance in removing subgroup disparity was on par with GDRO with group adjustment (Table 4) while delivering significantly higher average and worst-group AUCs (Table 3).

Conclusions and Discussion: We presented an evaluation study that derived important new insights into the working mechanisms and limitations of DRO and invariant representation learning to address spurious correlation caused by underrepresentation. The findings motivated us to present a novel approach that leverages robust optimization to facilitate the learning of invariant representations at the presence of spurious correlations. Finetuned classifiers utilizing

such representation demonstrated an improved ability to reduce subgroup performance disparity while maintaining high average and worst-group performance. Future investigations will include a broader spectrum of approaches including those utilizing data augmentation, as well as extending to a wider range of medical image datasets exploring potential hidden biases.

4 Acknowledgments

This work is supported by the National Institute of Nursing Research (NINR) of the National Institutes of Health (NIH) under Award Number R01NR018301.

References

1. Ben-Tal, A., Den Hertog, D., De Waegenare, A., Melenberg, B., Rennen, G.: Robust solutions of optimization problems affected by uncertain probabilities. *Management Science* **59**(2), 341–357 (2013)
2. Codella, N., Rotemberg, V., Tschandl, P., Celebi, M.E., Dusza, S., Gutman, D., Helba, B., Kalloo, A., Liopyris, K., Marchetti, M., et al.: Skin lesion analysis toward melanoma detection 2018: A challenge hosted by the international skin imaging collaboration (isic). arXiv preprint arXiv:1902.03368 (2019)
3. Deng, W., Zhong, Y., Dou, Q., Li, X.: On fairness of medical image classification with multiple sensitive attributes via learning orthogonal representations. In: *International Conference on Information Processing in Medical Imaging*. pp. 158–169. Springer (2023)
4. Ganin, Y., Ustinova, E., Ajakan, H., Germain, P., Larochelle, H., Laviolette, F., Marchand, M., Lempitsky, V.: Domain-adversarial training of neural networks (2015). <https://doi.org/10.48550/ARXIV.1505.07818>, <https://arxiv.org/abs/1505.07818>
5. Goel, K., Gu, A., Li, Y., Ré, C.: Model patching: Closing the subgroup performance gap with data augmentation. arXiv preprint arXiv:2008.06775 (2020)
6. Groh, M., Harris, C., Soenksen, L., Lau, F., Han, R., Kim, A., Koochek, A., Badri, O.: Evaluating deep neural networks trained on clinical images in dermatology with the fitzpatrick 17k dataset. In: *Proceedings of the IEEE/CVF Conference on Computer Vision and Pattern Recognition*. pp. 1820–1828 (2021)
7. He, K., Zhang, X., Ren, S., Sun, J.: Deep residual learning for image recognition. In: *Proceedings of the IEEE conference on computer vision and pattern recognition*. pp. 770–778 (2016)
8. Jiménez-Sánchez, A., Juodelye, D., Chamberlain, B., Cheplygina, V.: Detecting shortcuts in medical images—a case study in chest x-rays. arXiv preprint arXiv:2211.04279 (2022)
9. Kinyanjui, N.M., Odonga, T., Cintas, C., Codella, N.C., Panda, R., Sattigeri, P., Varshney, K.R.: Fairness of classifiers across skin tones in dermatology. In: *Medical Image Computing and Computer Assisted Intervention—MICCAI 2020: 23rd International Conference, Lima, Peru, October 4–8, 2020, Proceedings, Part VI*. pp. 320–329. Springer (2020)
10. Kirichenko, P., Izmailov, P., Wilson, A.G.: Last layer re-training is sufficient for robustness to spurious correlations. arXiv preprint arXiv:2204.02937 (2022)

11. Kohonen, T.: The self-organizing map. *Proceedings of the IEEE* **78**(9), 1464–1480 (1990)
12. Liu, E.Z., Haghgoo, B., Chen, A.S., Raghunathan, A., Koh, P.W., Sagawa, S., Liang, P., Finn, C.: Just train twice: Improving group robustness without training group information. In: Meila, M., Zhang, T. (eds.) *Proceedings of the 38th International Conference on Machine Learning. Proceedings of Machine Learning Research*, vol. 139, pp. 6781–6792. PMLR (18–24 Jul 2021), <https://proceedings.mlr.press/v139/liu21f.html>
13. Louizos, C., Swersky, K., Li, Y., Welling, M., Zemel, R.: The variational fair autoencoder (2015). <https://doi.org/10.48550/ARXIV.1511.00830>, <https://arxiv.org/abs/1511.00830>
14. McCoy, T., Pavlick, E., Linzen, T.: Right for the wrong reasons: Diagnosing syntactic heuristics in natural language inference. In: *Proceedings of the 57th Annual Meeting of the Association for Computational Linguistics*. pp. 3428–3448. Association for Computational Linguistics, Florence, Italy (Jul 2019). <https://doi.org/10.18653/v1/P19-1334>, <https://aclanthology.org/P19-1334>
15. Nam, J., Cha, H., Ahn, S., Lee, J., Shin, J.: Learning from failure: De-biasing classifier from biased classifier. *Advances in Neural Information Processing Systems* **33**, 20673–20684 (2020)
16. Oakden-Rayner, L., Dunnmon, J., Carneiro, G., Ré, C.: Hidden stratification causes clinically meaningful failures in machine learning for medical imaging. In: *Proceedings of the ACM conference on health, inference, and learning*. pp. 151–159 (2020)
17. Park, S., Hwang, S., Kim, D., Byun, H.: Learning disentangled representation for fair facial attribute classification via fairness-aware information alignment. In: *Proceedings of the AAAI Conference on Artificial Intelligence*. vol. 35, pp. 2403–2411 (2021)
18. Rajpurkar, P., Irvin, J., Zhu, K., Yang, B., Mehta, H., Duan, T., Ding, D., Bagul, A., Langlotz, C., Shpanskaya, K., et al.: Chexnet: Radiologist-level pneumonia detection on chest x-rays with deep learning. *arXiv preprint arXiv:1711.05225* (2017)
19. Rieger, L., Singh, C., Murdoch, W., Yu, B.: Interpretations are useful: penalizing explanations to align neural networks with prior knowledge. In: *International conference on machine learning*. pp. 8116–8126. PMLR (2020)
20. Sagawa, S., Koh, P.W., Hashimoto, T.B., Liang, P.: Distributionally robust neural networks for group shifts: On the importance of regularization for worst-case generalization. *arXiv preprint arXiv:1911.08731* (2019)
21. Sarhan, M.H., Navab, N., Eslami, A., Albarqouni, S.: Fairness by learning orthogonal disentangled representations. In: *Computer Vision—ECCV 2020: 16th European Conference, Glasgow, UK, August 23–28, 2020, Proceedings, Part XXIX* 16. pp. 746–761. Springer (2020)
22. Sohoni, N., Dunnmon, J., Angus, G., Gu, A., Ré, C.: No subclass left behind: Fine-grained robustness in coarse-grained classification problems. *Advances in Neural Information Processing Systems* **33**, 19339–19352 (2020)
23. Vapnik, V.: Principles of risk minimization for learning theory. *Advances in neural information processing systems* **4** (1991)
24. Wang, H., He, Z., Lipton, Z.C., Xing, E.P.: Learning robust representations by projecting superficial statistics out. *arXiv preprint arXiv:1903.06256* (2019)
25. Wu, Y., Zeng, D., Xu, X., Shi, Y., Hu, J.: Fairprune: Achieving fairness through pruning for dermatological disease diagnosis. In: Wang, L., Dou, Q., Fletcher, P.T., Speidel, S., Li, S. (eds.) *Medical Image Computing and Computer Assisted Intervention – MICCAI 2022*. pp. 743–753. Springer Nature Switzerland, Cham (2022)

26. Zhang, M., Sohoni, N.S., Zhang, H.R., Finn, C., Re, C.: Correct-n-contrast: a contrastive approach for improving robustness to spurious correlations. In: Chaudhuri, K., Jegelka, S., Song, L., Szepesvari, C., Niu, G., Sabato, S. (eds.) Proceedings of the 39th International Conference on Machine Learning. Proceedings of Machine Learning Research, vol. 162, pp. 26484–26516. PMLR (17–23 Jul 2022), <https://proceedings.mlr.press/v162/zhang22z.html>
27. Zhao, Q., Adeli, E., Pohl, K.M.: Training confounder-free deep learning models for medical applications. *Nature communications* **11**(1), 6010 (2020)

Distributionally Robust Optimization and Invariant Representation Learning for Addressing Subgroup Underrepresentation: Mechanisms and Limitations: Supplemental Document

Nilesh Kumar*, Ruby Shrestha*, Zhiyuan Li and Linwei Wang

Rochester Institute of Technology, NY, USA

1 SOM Purity Values for ISIC and Fitzpatrick Datasets

1.1 ISIC Dataset

	Benign, No Bandage	Benign, Bandage	Malignant, No Bandage	Malignant, Bandage	Average
ERM	0.763 ± 0.024	0.945 ± 0.007	0.823 ± 0.024	0.730 ± 0.014	0.815 ± 0.010
GDRO	0.768 ± 0.088	0.953 ± 0.010	0.763 ± 0.052	0.710 ± 0.090	0.798 ± 0.015
GDRO with group adjustment	0.803 ± 0.061	0.973 ± 0.000	0.725 ± 0.049	0.743 ± 0.004	0.811 ± 0.029
DANN	0.802 ± 0.040	0.940 ± 0.057	0.775 ± 0.106	0.746 ± 0.019	0.816 ± 0.007
Proposed method	0.685 ± 0.021	0.830 ± 0.028	0.755 ± 0.007	0.620 ± 0.014	0.723 ± 0.007

Table 1. SOM purities for subgroups in ISIC dataset. The proposed method resulted in the least biases in latent representations on average and for almost all the subgroups with either the lowest or the second-lowest SOM purity measures. Best performance is shaded gray, with bolded performance coming closely behind.

1.2 Fitzpatrick Dataset

	Malignant-1,2	Malignant-5,6	Non-neoplastic-1,2	Non-neoplastic-5,6	Average
ERM	0.615 ± 0.031	0.500 ± 0.000	0.915 ± 0.011	0.624 ± 0.034	0.664 ± 0.019
GDRO	0.555 ± 0.008	0.459 ± 0.059	0.902 ± 0.013	0.648 ± 0.000	0.641 ± 0.016
GDRO with group adjustment	0.588 ± 0.008	0.500 ± 0.000	0.895 ± 0.007	0.673 ± 0.025	0.664 ± 0.006
DANN	0.593 ± 0.062	0.459 ± 0.059	0.908 ± 0.015	0.597 ± 0.005	0.639 ± 0.004
Proposed method	0.571 ± 0.016	0.271 ± 0.088	0.899 ± 0.012	0.583 ± 0.015	0.581 ± 0.027

Table 2. SOM purities for subgroups in Fitzpatrick dataset. In Fitzpatrick dataset as well, the proposed method resulted in the least biases in latent representations on average and for almost all the subgroups with either the lowest or the second-lowest SOM purity measures.

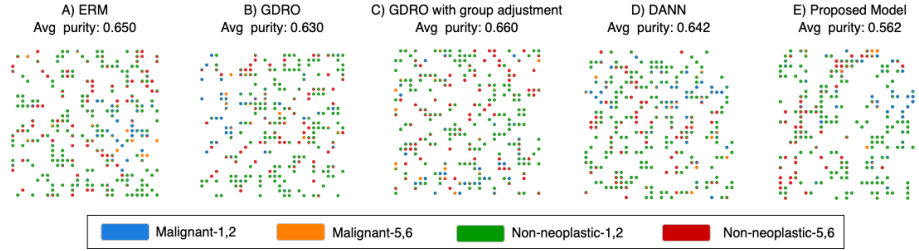


Fig. 1. SOM plots and averaged subgroup purities for Fitzpatrick dataset. Malignant-1,2/-5,6 and Non-neoplastic-1,2/-5,6 are the subgroups where the bias primarily exists.

2 Complete Performance on Fitzpatrick Dataset

Methods	Benign Skin Types						$\Delta_{best-worst}$
	1	2	3	4	5	6	
ERM	0.770 \pm 0.020	0.723 \pm 0.015	0.780 \pm 0.026	0.757 \pm 0.040	0.837 \pm 0.049	0.617 \pm 0.040	0.223 \pm 0.032
Importance weighting	0.747 \pm 0.031	0.673 \pm 0.035	0.767 \pm 0.029	0.747 \pm 0.029	0.827 \pm 0.031	0.697 \pm 0.015	0.153 \pm 0.006
DANN	0.710 \pm 0.010	0.680 \pm 0.010	0.743 \pm 0.006	0.763 \pm 0.012	0.840 \pm 0.010	0.607 \pm 0.015	0.233 \pm 0.015
DFR	0.727 \pm 0.012	0.673 \pm 0.015	0.757 \pm 0.025	0.757 \pm 0.032	0.810 \pm 0.010	0.687 \pm 0.059	0.137 \pm 0.015
GDRO	0.733 \pm 0.032	0.673 \pm 0.035	0.777 \pm 0.015	0.750 \pm 0.020	0.837 \pm 0.031	0.700 \pm 0.082	0.197 \pm 0.055
GDRO with group adjustment	0.703 \pm 0.015	0.647 \pm 0.006	0.723 \pm 0.021	0.710 \pm 0.017	0.810 \pm 0.020	0.710 \pm 0.036	0.163 \pm 0.021
Proposed method	0.753 \pm 0.006	0.697 \pm 0.006	0.797 \pm 0.006	0.753 \pm 0.006	0.787 \pm 0.006	0.690 \pm 0.035	0.117 \pm 0.031

Table 3. AUC values of individual skin types in the Benign category. The proposed method performed the best in removing the overall subgroup disparity. Best performance is shaded gray, with bolded performance coming closely behind.

Methods	Malignant Skin Types						$\Delta_{best-worst}$
	1	2	3	4	5	6	
ERM	0.887 \pm 0.012	0.870 \pm 0.010	0.867 \pm 0.021	0.830 \pm 0.010	0.873 \pm 0.006	0.747 \pm 0.032	0.140 \pm 0.026
Importance weighting	0.893 \pm 0.015	0.863 \pm 0.006	0.897 \pm 0.006	0.873 \pm 0.015	0.880 \pm 0.010	0.827 \pm 0.015	0.073 \pm 0.021
DANN	0.863 \pm 0.012	0.850 \pm 0.010	0.840 \pm 0.000	0.783 \pm 0.015	0.883 \pm 0.006	0.633 \pm 0.032	0.250 \pm 0.036
DFR	0.877 \pm 0.006	0.850 \pm 0.010	0.870 \pm 0.017	0.813 \pm 0.006	0.890 \pm 0.010	0.737 \pm 0.038	0.153 \pm 0.046
GDRO	0.877 \pm 0.006	0.860 \pm 0.010	0.883 \pm 0.021	0.850 \pm 0.017	0.887 \pm 0.006	0.810 \pm 0.104	0.090 \pm 0.087
GDRO with group adjustment	0.863 \pm 0.006	0.840 \pm 0.010	0.893 \pm 0.006	0.850 \pm 0.000	0.887 \pm 0.006	0.867 \pm 0.029	0.053 \pm 0.015
Proposed method	0.897 \pm 0.006	0.870 \pm 0.000	0.883 \pm 0.006	0.853 \pm 0.012	0.867 \pm 0.006	0.807 \pm 0.006	0.090 \pm 0.010

Table 4. AUC values of individual skin types in the Malignant category. The proposed method delivered improvement over DANN in reducing the overall subgroup disparity and it was the third-best method in terms of $\Delta_{best-worst}$.

Methods	Non-neoplastic Skin Types						$\Delta_{best-worst}$
	1	2	3	4	5	6	
ERM	0.777 \pm 0.015	0.777 \pm 0.006	0.810 \pm 0.010	0.837 \pm 0.012	0.857 \pm 0.006	0.853 \pm 0.006	0.083 \pm 0.015
Importance weighting	0.780 \pm 0.010	0.780 \pm 0.010	0.800 \pm 0.010	0.833 \pm 0.015	0.847 \pm 0.006	0.860 \pm 0.017	0.080 \pm 0.020
DANN	0.790 \pm 0.010	0.780 \pm 0.000	0.803 \pm 0.006	0.820 \pm 0.010	0.807 \pm 0.015	0.793 \pm 0.015	0.040 \pm 0.010
DFR	0.780 \pm 0.010	0.777 \pm 0.006	0.800 \pm 0.010	0.823 \pm 0.006	0.830 \pm 0.010	0.827 \pm 0.012	0.053 \pm 0.006
GDRO	0.793 \pm 0.015	0.783 \pm 0.012	0.797 \pm 0.012	0.813 \pm 0.015	0.817 \pm 0.031	0.833 \pm 0.012	0.053 \pm 0.025
GDRO with group adjustment	0.787 \pm 0.015	0.777 \pm 0.015	0.773 \pm 0.012	0.793 \pm 0.006	0.780 \pm 0.020	0.797 \pm 0.025	0.030 \pm 0.010
Proposed method	0.807 \pm 0.006	0.800 \pm 0.000	0.800 \pm 0.000	0.837 \pm 0.006	0.827 \pm 0.006	0.833 \pm 0.012	0.037 \pm 0.006

Table 5. AUC values of individual skin types in the Non-neoplastic category. The proposed method was the only one that decreased the bias against Non-neoplastic skin types 1 and 2. Also, its performance in removing overall subgroup disparity was on par with GDRO with group adjustment and was better than DANN.